Acta Crystallographica Section F
**Structural Biology and Crystallization Communications**
ISSN 1744-3091

# Water-mediated variability in the structure of relaxed-state haemoglobin

**Prem Singh Kaushal, R. Sankaranarayanan and M. Vijayan***

Molecular Biophysics Unit, Indian Institute of Science, Bangalore 560 012, India

Correspondence e-mail: mv@mbu.iisc.ernet.in

Received 6 March 2008
Accepted 3 May 2008

**PDB References:** methaemoglobin, native, 2zlt, r2zltsf; 88% r.h., 2zlu, r2zlusf; 79% r.h., 2zlv, r2zlvsf; 75% r.h., 2zlw, r2zlwsf; 66% r.h., 2zlx, r2zlxsf.

The crystal structure of high-salt horse methaemoglobin has been determined at environmental relative humidities (r.h.) of 88, 79, 75 and 66%. The molecule is in the R state in the native and the r.h. 88% crystals. At r.h. 79%, the water content of the crystal is reduced and the molecule appears to move towards the R2 state. The crystals undergo a water-mediated transformation involving a doubling of one of the unit-cell parameters and an increase in water content when the environmental humidity is further reduced to r.h. 75%. The water content is now similar to that in the native crystals and the molecules are in the R state. The crystal structure at r.h. 66% is similar, but not identical, to that at r.h. 75%, but the solvent content is substantially reduced and the molecules have a quaternary structure that is in between those corresponding to the R and R2 states. Thus, variation in hydration leads to variation in the quaternary structure. Furthermore, partial dehydration appears to shift the structure from the R state to the R2 state. This observation is in agreement with the earlier conclusion that the changes in protein structure that accompany partial dehydration are similar to those that occur during protein action.

## 1. Introduction

Tetrameric haemoglobin was one of the first two protein structures to be determined by X-ray crystallography. It has also remained the most important system for investigating allostery in protein action. The explanation by Perutz of the stereochemical mechanisms of the cooperative effects in haemoglobin (Perutz, 1970; Perutz *et al.*, 1998) closely followed the model of allosteric transitions proposed by Monod, Wyman and Changeux (Monod *et al.*, 1965). It involved the transition between a fully oxygenated 'relaxed' R state and a fully deoxygenated 'tense' T state, both involving the ferrous ion in the prosthetic haem group. The molecule with the haem carrying a ferric ion (methaemoglobin) and those with carbon monoxide, water *etc.* as bound ligands also exist in the R state. Much of the early work by Perutz and others was performed on horse haemoglobin. Subsequently, attention shifted to human haemoglobin (Baldwin, 1980; Shaanan, 1983; Fermi *et al.*, 1984; Brzozowski *et al.*, 1984; Liddington *et al.*, 1992; Silva *et al.*, 1992; Vásquez *et al.*, 1998; Biswal & Vijayan, 2001, 2002; Safo & Abraham, 2005; Park *et al.*, 2006). Interestingly, a new relaxed state, termed R2 (Silva *et al.*, 1992), was discovered in the human protein. Later, the structural analysis in this laboratory of human methaemoglobin using crystals containing three crystallographically independent tetramers demonstrated that relaxed haemoglobin can exist in an ensemble of states with varying degrees of similarity to R and R2 (Biswal & Vijayan, 2001). Simultaneously, a similar conclusion was arrived at elsewhere through studies on liganded bovine haemoglobin (Mueser *et al.*, 2000). A subsequent study by us showed that the deoxy form of haemoglobin can also access an ensemble of related T states (Biswal & Vijayan, 2002). A recent study on carbonmonoxyhaemoglobin has led to the identification of another relaxed state christened R3 (Safo & Abraham, 2005).

Until recently, no relaxed state other than R had been observed in horse haemoglobin. However, we recently characterized horse

© 2008 International Union of Crystallography
All rights reserved

**Table 1**
Crystal data and data-collection, refinement and model statistics.

Values in parentheses are for the highest resolution shell.

| | Native | R.h. 88% | R.h. 79% | R.h 75% | R.h. 66% |
|---|---|---|---|---|---|
| Space group | *C*2 | *C*2 | *C*2 | *C*2 | *C*2 |
| Unit-cell parameters | | | | | |
| *a* (Å) | 108.65 | 108.18 | 94.10 | 108.27 | 108.44 |
| *b* (Å) | 63.34 | 63.34 | 62.94 | 63.27 | 63.40 |
| *c* (Å) | 54.96 | 54.41 | 53.16 | 108.15 | 102.59 |
| *β* (°) | 110.8 | 111.1 | 115.3 | 111.3 | 121.0 |
| Unit-cell volume (Å$^3$) | 353578 | 347827 | 284649 | 690306.75 | 604735 |
| *Z* | 2 | 2 | 2 | 4 | 4 |
| Solvent content (%) | 54.9 | 54.2 | 44.0 | 53.8 | 47.3 |
| Data resolution (Å) | 20.0–1.9 (1.97–1.9) | 20.0–2.0 (2.07–2.0) | 20.0–2.0 (2.07–2.0) | 20.0–2.9 (3.0–2.9) | 20.0–2.8 (2.9–2.8) |
| No. of observed reflections | 94436 | 58131 | 59746 | 18235 | 17768 |
| No. of unique reflections | 26933 (2725) | 22583 (2140) | 18738 (1887) | 14192 (1443) | 11560 (1227) |
| Multiplicity | 3.5 | 2.6 | 3.2 | 1.3 | 1.5 |
| Completeness of data (%) | 97.6 (99.8) | 96.8 (92.0) | 98.2 (99.4) | 92.9 (94.5) | 77.7 (82.2) |
| $R_{merge}$† (%) | 13.6 (52.8) | 10.6 (44.5) | 12.6 (39.3) | 18.5 (37.8) | 17.3 (34.4) |
| Average $I/\sigma(I)$ | 8.7 (3.3) | 7.3 (2.5) | 7.7 (2.8) | 4.6 (2.7) | 3.2 (2.1) |
| *R* factor (%) | 19.0 | 19.3 | 19.8 | 27.4 | 26.0 |
| $R_{free}$‡ (%) | 22.6 | 22.2 | 23.0 | 29.4 | 29.3 |
| Protein atoms | 2169 | 2176 | 2109 | 4390 | 4272 |
| Solvent atoms | 216 | 164 | 151 | — | — |
| Haem atoms | 86 | 86 | 86 | 172 | 172 |
| R.m.s. deviation from ideal values | | | | | |
| Bond lengths (Å) | 0.013 | 0.014 | 0.017 | 0.014 | 0.012 |
| Bond angles (°) | 1.2 | 1.3 | 1.3 | 1.5 | 1.5 |
| Residues (%) in Ramachandran plot§ | | | | | |
| Core regions | 92.3 | 93.1 | 92.4 | 83.7 | 82.8 |
| Additionally allowed regions | 7.3 | 6.5 | 7.6 | 15.1 | 16.4 |
| Generously allowed regions | 0.4 | 0.4 | 0.0 | 1.2 | 0.4 |
| Disallowed regions | 0.0 | 0.0 | 0.0 | 0.0 | 0.4 |

† $R_{merge} = \sum_{hkl}\sum_i |I_i(hkl) - \langle I(hkl)\rangle| / \sum_{hkl}\sum_i I_i(hkl)$, where $I_i(hkl)$ is the *i*th observation of reflection *hkl* and $\langle I(hkl)\rangle$ is the weighted average intensity for all observations *i* of reflection *hkl*. ‡ 5% of reflections were used for the $R_{free}$ calculations. § Calculated for nonglycine and nonproline residues using *PROCHECK*.

methaemoglobin molecules in states between R and R2 using crystals grown at neutral pH with polyethylene glycol as the precipitant (Sankaranarayanan *et al.*, 2005). Here, we examine the original high-salt crystals of horse methaemoglobin grown at neutral pH at different levels of water content. Preliminary studies of this nature examining crystals in environments involving different relative humidities were carried out by Perutz, Kendrew and others (Perutz, 1954; Huxley & Kendrew, 1953) in the middle of the last century. Protein crystallography was at a primitive stage at that time and the structural ramifications of the preliminary results were not further pursued. Subsequently, water-mediated transformations, in which protein crystals undergo reversible transformations accompanied by change in water content when the environmental humidity is systematically varied, were developed by us into a tool for investigating protein hydration and its consequences, particularly in relation to molecular plasticity and protein action (Salunke *et al.*, 1985). Specifically, it was demonstrated in the case of lysozyme (Kodandapani *et al.*, 1990; Madhusudan *et al.*, 1991, 1993; Nagendra *et al.*, 1996, 1998; Sukumar *et al.*, 1999; Biswal *et al.*, 2000) and ribonuclease A (Radha Kishan *et al.*, 1995; Sadasivan *et al.*, 1998) that the structural changes that accompany partial dehydration are similar to those that occur during enzyme action, thus establishing a relationship between hydration, plasticity and protein action. Somewhat similar results were also obtained recently in the case of *β*-lactoglobulin (Vijayalakshmi *et al.*, 2008). Our current investigation of haemoglobin involves, to a substantial extent, an attempt to apply the approach involving variation in water content and water-mediated transformations to larger and more complex systems. The results obtained so far have been very satisfactory. In the work reported here, we demonstrate how relaxed states between R and R2 can be generated by simply changing the amount of water surrounding the crystals. The results also appear to suggest that partial dehydration pushes the equilibrium toward R2, which is described as an end state (Srinivasan & Rose, 1994; Schumacher *et al.*, 1997).

## 2. Materials and methods

### 2.1. Crystallization, X-ray data collection and processing

Lyophilized powdered horse methaemoglobin was purchased from Sigma Chemical Company. A 20 mg ml$^{-1}$ protein solution was dialyzed against 0.01 *M* ammonium phosphate buffer pH 7.0 prior to crystallization. Crystals were grown following the procedure described by Perutz (1968). A mixture of 2 ml 20 mg ml$^{-1}$ protein solution and 3 ml solution *B* [two volumes of 4 *M* $(NH_4)_2SO_4$ and one volume of phosphate buffer consisting of 0.95 volume 2 *M* $(NH_4)_2HPO_4$ and 0.05 volume 2 *M* $(NH_4)H_2PO_4$] was used in a batch method. To maintain the environmental humidity (r.h.) at 88, 79, 75 and 66%, supersaturated salt solutions of $K_2CrO_4$, $NH_4Cl$, $NaClO_3$ and $NaNO_2$ (West & Astle, 1980), respectively, were placed at a distance of about 1 cm from the crystal in a glass capillary before sealing. The salt solution never comes into contact with the crystal. This maintains the r.h. at the desired value within the sealed capillary. After 24 h of equilibration, intensity data collection was performed. The data were collected from the native, the r.h. 88%, the r.h. 79%, the r.h. 75% and the r.h. 66% forms on a MAR imaging plate mounted on a Rigaku RU-200 rotating copper-anode X-ray generator. The diffraction data sets were processed and scaled using *DENZO* and *SCALEPACK* (Otwinowski & Minor, 1997). Intensities were converted to structure-factor amplitudes using *TRUNCATE* (Collaborative Computational Project, Number 4, 1994).

It was extremely difficult to obtain crystals maintained at r.h. 75% and r.h. 66%. Most often a diffraction pattern could not be indexed from the crystals at r.h. 75%. To start with, the crystals maintained at

r.h. 66% did not diffract at all or exhibited unacceptably high mosaicity. Subsequently, r.h. 66% crystals were obtained in a two-step process. Initially, crystals were maintained at r.h. 79% for 24 h using a saturated solution of $NH_4Cl$. This solution was then carefully removed and replaced by a saturated solution of $NaNO_2$ to obtain an environmental r.h. of 66%. Even then, reasonable diffraction patterns were only rarely obtained. Nevertheless, when obtained, the pattern could be indexed and the data could be processed. However, the life of the crystal in the X-ray beam was short at r.h. 75% and r.h. 66%. Consequently, the data completeness is poor, particularly at r.h. 66%. Despite this, the results obtained using the data sets are good enough to describe the crystal structures and gross changes in quaternary associations, which forms the main theme of this paper.

### 2.2. Structure solution and refinement

The structure of horse methaemoglobin (PDB code 2mhb; 2.0 Å resolution) was used as the initial model for refinement of the native and the r.h. 88% forms. The r.h. 79%, the r.h. 75% and the r.h. 66% forms were solved using the molecular-replacement program *AMoRe* (Navaza, 1994). The structure of horse methaemoglobin (2mhb) was used as a search model. *AMoRe* yielded best solutions with correlation coefficients of 54.4, 59.5 and 52.4 and *R* factors of 35.0, 44.2 and 46.2% for the r.h. 79%, the r.h. 75% and the r.h. 66% forms, respectively. All the structures were initially refined using *CNS* v.1.1 incorporating the maximum-likelihood target (Brünger *et al.*, 1998). Refinement using a tetramer, a dimer and a subunit as rigid bodies was followed by atomic position and *B*-factor refinement. At this stage electron-density maps were calculated and model building was performed manually using the program *O* (Jones *et al.*, 1991). After each cycle of model building, atomic position and *B*-factor refinements were carried out. Water molecules were identified, except in the r.h. 75% and r.h. 66% forms, initially at peaks greater than $3\sigma$ in $F_o - F_c$ maps and $1\sigma$ in $2F_o - F_c$ maps. Subsequently, the threshold values were lowered to $2.5\sigma$ in $F_o - F_c$ and $0.8\sigma$ in $2F_o - F_c$ maps, respectively. Cycles of positional and *B*-factor refinement, correction of the model using Fourier maps and the search for locations of water molecules were continued until no further significant density remained in the maps. The structural parameters of the haem group (Kuriyan *et al.*, 1986) as well as the protein molecule were restrained in order to maintain proper geometry. The final cycles of refinement were carried out using the program *REFMAC* (Murshudov *et al.*, 1997) in *CCP*4 (Collaborative Computational Project, Number 4, 1994). Stereochemical parameters were checked using *PROCHECK* (Laskowski *et al.*, 1993). Molecular superpositions were performed using *ALIGN* (Cohen, 1997). Figures were generated using the programs *PyMOL* (DeLano, 2002), *MOLSCRIPT* (Kraulis, 1991) and *RASTER3D* (Merritt & Bacon, 1997). Crystal data and data-collection, refinement and model statistics are given in Table 1. The 43–56 stretch in the $\beta$-chain is not defined in the r.h. 79% form. No major disorder in main-chain atoms is found in the other forms.

## 3. Results

### 3.1. Water content, transformation and crystal packing

The crystals have been examined under native conditions and at environmental relative humidities (r.h.) of 88, 79, 75 and 66%. The water content of the crystals, estimated using the method of Matthews (1968), and molecular packing are not linearly related to environmental humidity (Fig. 1). The water contents of the native crystals and crystals in an environment of r.h. 88% are nearly the same. However, the water content reduces substantially when the r.h. is reduced to 79%. Further reduction of the r.h. to 75%, however, results in an increase in water content. This reduction in r.h. is also accompanied by a transformation. The water content reduces from this point when the environmental humidity is further reduced.

The unit-cell parameters at different levels of r.h. are illustrated in Fig. 2. The unique axis *b* has nearly the same length at all humidity levels. The unit-cell parameters are very nearly the same in the native crystals and in those at r.h. 88%. By the time the r.h. is reduced to 75%, the crystals have undergone a transformation with a doubling (with respect to the native crystals) of the *c* axis, as seen in the preliminary observations in 1954 (Huxley & Kendrew, 1953). This involves a change in the molecular packing and consequent changes in the unit-cell parameters. The length of the *a* axis is restored to that in the native crystals. At r.h. 66%, the *a* parameter remains the same. The length of *c* decreases substantially, with an increase in the monoclinic angle.

The crystal packing is essentially the same in the native crystals and at r.h. 88% and r.h. 79%. The haemoglobin molecules are situated on crystallographic twofold axes with an $\alpha\beta$ dimer in the asymmetric unit (Fig. 3). The twofold axes on which the molecules are located are at $a = 0$, $c = 0$ and $a = \frac{1}{2}$, $c = 0$ and their translational equivalents. The dyads at $a = 0$, $c = \frac{1}{2}$ and $a = \frac{1}{2}$, $c = \frac{1}{2}$ and their translational equivalents relate adjacent tetrameric molecules. The transitions resulting from a further reduction in r.h. lead to not only the doubling of the *c* axis but

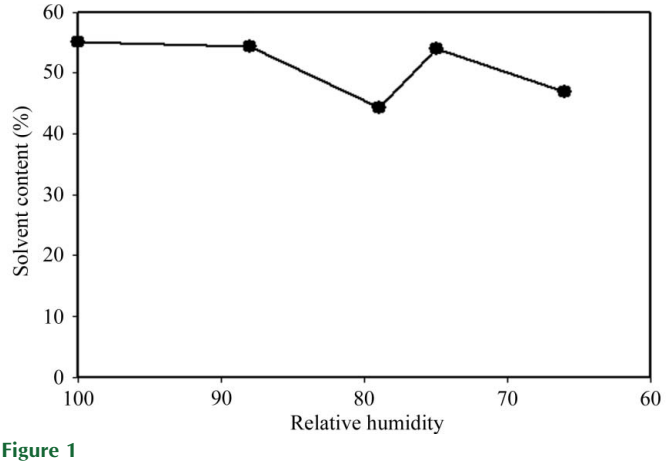


**Figure 1**
Variation of solvent content as a function of relative humidity.

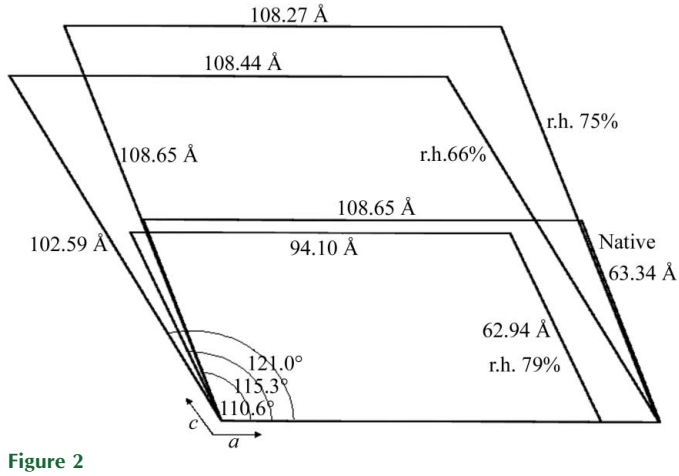


**Figure 2**
Unit cells of the native, the r.h. 79%, the r.h. 75% and the r.h. 66% forms of horse methaemoglobin crystals viewed along the *b* axis.

also to the disappearance of one set of twofold axes. The space group remains the same (*C*2). However, surprisingly, the twofold axes that disappear are different at r.h. 75% and r.h. 66%. Consequently, the arrangement of molecules is also different in the two forms. The twofold axes that disappear at r.h. 75% are those that relate the two halves of the tetrameric molecules in the native crystals. Consequently, there is now one tetrameric molecule in the asymmetric unit. In contrast, the twofold axes that disappear at r.h. 66% are those which relate neighbouring tetramers. Therefore, in this form there are two half tetramers in the asymmetric unit. Each tetramer occupies a crystallographic dyad. Thus, the crystal structures at r.h. 75% and r.h. 66% are distinctly different, although similar in a subtle way. It does not appear that the r.h. 66% form passes through the r.h. 75% phase. It is possible that both forms occur when the transformation takes place, with one form tending to predominate at r.h. 75% and the other predominating at r.h. 66%. One has a crystallographically independent tetramer while the other has two, but each with crystallographic twofold symmetry.

The uptake of water during the transformation from the r.h. 79% form to the r.h. 75% form is counterintuitive and merits an explanation. As illustrated in Fig. 4(*a*), the 38–48 loop in the $\alpha$-chain, the 39–58 stretch in the $\beta$-chain and the C-terminal region of the $\alpha$76–91

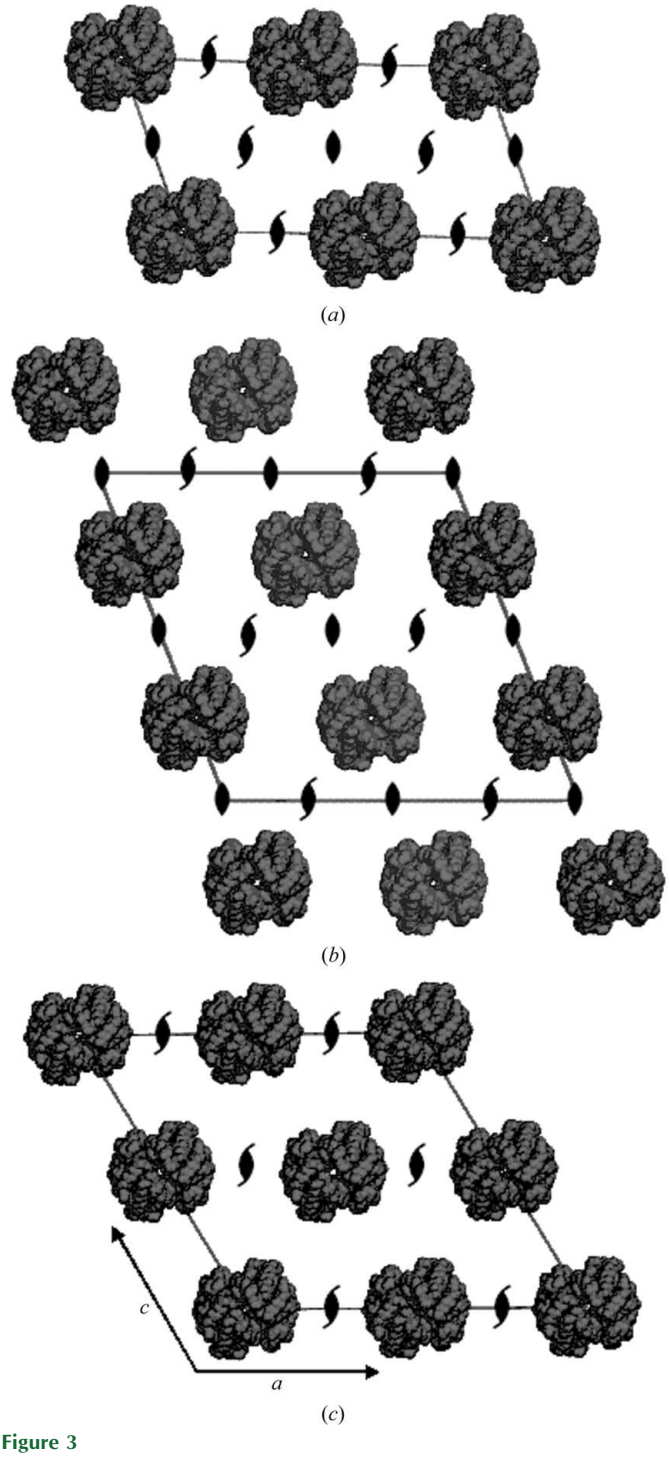


**Figure 3**
The crystal packing in (*a*) the native, (*b*) the r.h. 75% and (*c*) the r.h. 66% forms. For clarity, the twofold axes that relate the two halves of the molecule in the native and the r.h. 66% forms are not shown.

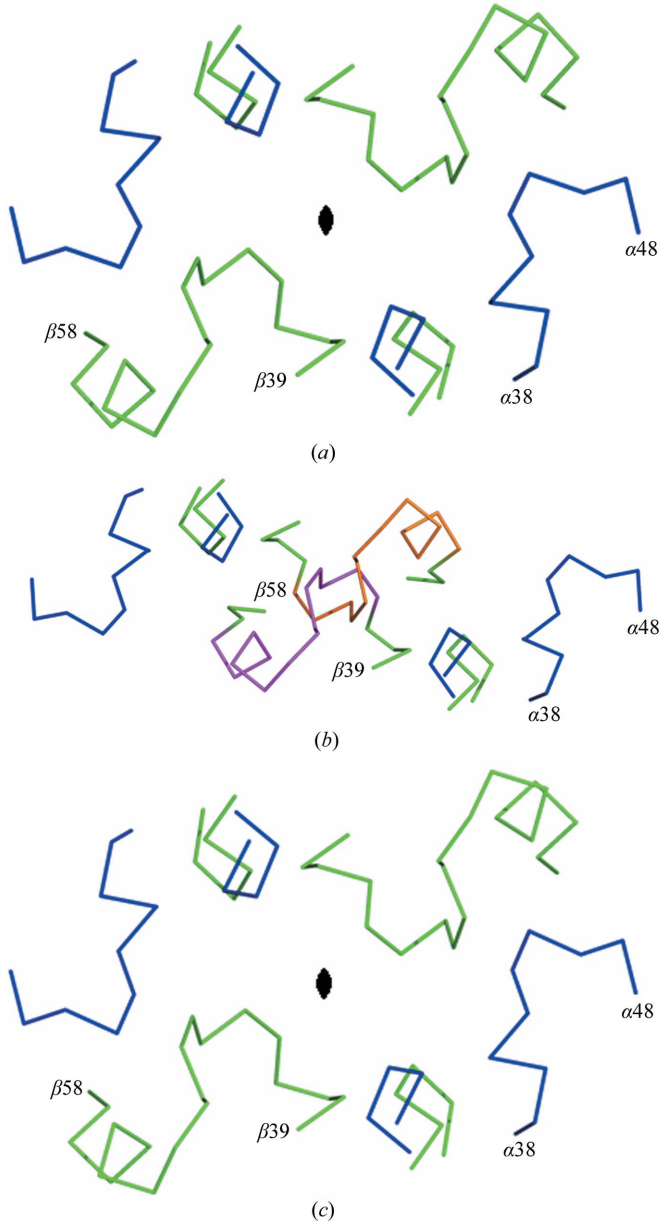


**Figure 4**
The interface between the two molecules related by a twofold axis in (*a*) the native crystals, (*b*) the r.h. 79% form and (*c*) the r.h. 75% form. Two stretches, one from the $\alpha$1 subunit (blue) and the other from the $\beta$2 subunit (green), are labelled. In (*b*), the disordered regions (magenta and orange) are modelled on the basis of the native structure and the twofold axis is not indicated for clarity. See text for details.

**Table 2**
R.m.s. deviations (Å) in the main-chain atoms resulting from the superposition of the $\alpha1\beta1$ subunits of pairs of molecules.

Deviations in the $\alpha1\beta1$ subunits are given in the lower left part of the table and those in the $\alpha2\beta2$ subunits in the upper right part. 1, native; 2, r.h. 79%; 3, r.h. 75%; 4, r.h. 66% molecule 1; 5, r.h. 66% molecule 2; 6, horse met low-salt r.h. 88% (PDB code 1y8k); 7, human R2 (1bbb); 8, horse deoxy T (2dhb).

| | 1 | 2 | 3 | 4 | 5 | 6 | 7 | 8 |
|---|---|---|---|---|---|---|---|---|
| 1 | — | 0.64 | 0.48 | 1.80 | 2.24 | 1.95 | 4.33 | 5.67 |
| 2 | 0.18 | — | 0.91 | 1.64 | 1.98 | 1.81 | 4.09 | 5.87 |
| 3 | 0.29 | 0.33 | — | 1.95 | 2.44 | 2.01 | 4.41 | 5.66 |
| 4 | 0.34 | 0.35 | 0.40 | — | 0.68 | 0.91 | 2.65 | 7.06 |
| 5 | 0.37 | 0.38 | 0.42 | 0.31 | — | 1.01 | 2.21 | 7.53 |
| 6 | 0.36 | 0.35 | 0.38 | 0.42 | 0.43 | — | 2.56 | 7.04 |
| 7 | 0.56 | 0.58 | 0.55 | 0.58 | 0.60 | 0.46 | — | 9.22 |
| 8 | 0.77 | 0.80 | 0.82 | 0.88 | 0.91 | 0.89 | 0.89 | — |

and $\beta$81–96 helices and their symmetry equivalents define the boundary of the water channel surrounding a crystallographic twofold axis. The size of the cross-section of the channel reduces when the solvent content is reduced. The reduction in water content is accompanied by a sliding motion between adjacent layers of molecules and a rotation of the molecules themselves. The sliding motion and the rotation are such that by the time the water content is as low as in the r.h. 79% form, the $\beta$43–$\beta$56 loop from one molecule collides with the same loop in the twofold-related molecule (Fig. 4*b*). This is presumably the reason for the disorder of this loop, which results from multiple conformations to avoid steric clash, in the r.h. 79% form. Any further reduction in the r.h. appears to render the packing arrangement unstable, leading to the uptake of water and the restoration of the monoclinic angle and the *a* dimension (Fig. 4*c*) as they existed in the native crystal. However, it is not clear why the *c* dimension doubles.

### 3.2. Changes in quaternary association

Five refined crystal structures are reported in the present study. The unit-cell parameters, solvent content and molecular structure of the native crystals and the r.h. 88% crystals are so similar that only the native crystals are considered in the present discussion. The native, the r.h. 79% and the r.h. 75% crystals contain one crystallographically independent molecule each, whereas the r.h. 66% crystals contain two crystallographically independent molecules. These five molecules are compared here amongst themselves and also with low-salt horse methaemoglobin (PDB code 1y8k), which may be described as the RR2 (intermediate between R and R2) state according to the nomenclature used recently (Safo & Abraham, 2005), T-state horse deoxyhaemoglobin (PDB code 2dhb) and R2-state human haemoglobin (PDB code 1bbb) (R2-state horse haemoglobin has not been observed to date). The native crystals in the present study are in the R state. The various RR2 structures observed to date (and in the present work) were obtained roughly by the rotation of half the molecule with respect to the other half about an axis that relates the R and R2 states by rotation. R3, however, is an independent relaxed state and is not included in the present discussion.

The tertiary structures of the $\alpha$ and $\beta$ subunits, including the environment of the haem, in all the structures reported here are nearly the same and correspond to those in the molecules in the relaxed state (Perutz, 1970; Perutz *et al.*, 1998; Silva *et al.*, 1992; Biswal & Vijayan, 2001; Safo & Abraham, 2005). However, differences exist in the quaternary structure. These are, as in all previously described cases, primarily caused by the rotation of one $\alpha\beta$ dimer with respect to the other. A rough-and-ready estimate of the differences in the quaternary structure of two haemoglobin molecules can be obtained by superposing the $\alpha1\beta1$ dimers of the two molecules and then looking for the root-mean-square (r.m.s.) deviations in the main-chain atoms between the $\alpha2\beta2$ dimers. Such deviations between pairs of structures considered in the present discussion are listed in Table 2. The movement of $\alpha2\beta2$ with respect to $\alpha1\beta1$ in a pair of molecules can also be described in terms of the angle $\theta_1$ between the molecular dyads in the two structures and a screw rotation angle $\theta_2$, the translation component of the screw, the direction of the screw rotation axis and a point on the rotation axis (Baldwin & Chothia, 1979). When calculating these parameters, the haemoglobin molecule was made perfectly twofold-symmetric as described previously (Biswal & Vijayan, 2001) whenever the molecular dyad did not coincide with crystallographic twofold axes. The angles $\theta_1$ and $\theta_2$ with respect to the native R structure for all the other structures considered here are illustrated in Fig. 5. These and other parameters for every pair of molecules are listed in Table 3.

Fig. 5 and Tables 2 and 3 clearly highlight the changes in quaternary structure that accompany removal of water from the crystal. The reduction in the solvent content with a marked shortening of the *a* axis from the native structure without any fundamental change in the crystal structure, as in the r.h. 79% form, results in a movement from the R to the R2 state. The water-mediated transformation that occurs between the r.h. 79% and r.h. 75% structures is accompanied by not only a change in crystal structure, with the disappearance of one set of twofold axes, but also in the uptake of water by the crystal. This increase in the level of hydration results in a movement back towards the R state. Further reduction of the environmental humidity results in a decreased solvent content as in the r.h. 66% from. The quaternary structures of the molecules in the

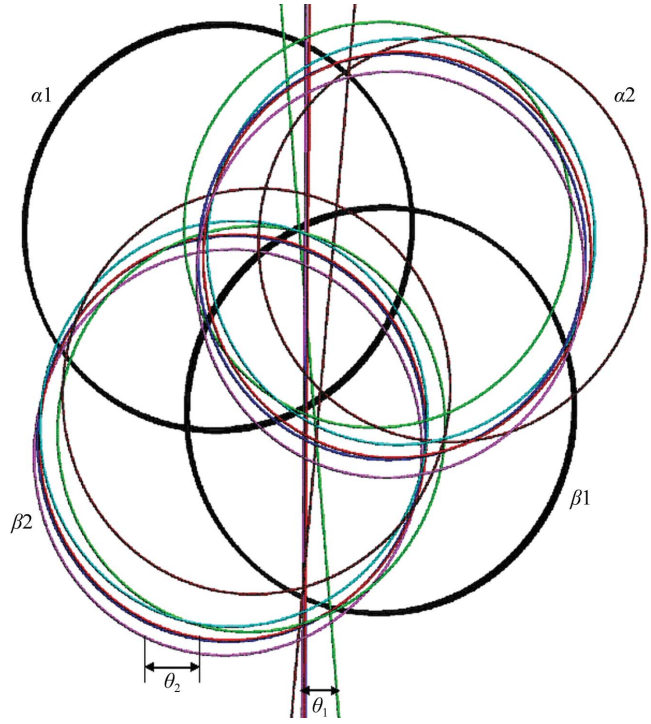


**Figure 5**
Schematic representation of selected haemoglobin quaternary structures. $\alpha1\beta1$ subunits of all structures are superimposed and are shown in black. The orientation of each nonsuperposed $\alpha2\beta2$ dimer is shown in a different colour: native (R), cyan; low-salt r.h. 88%, blue; r.h. 66% molecule 2, red; R2, violet; R3, green; deoxy (T), brown.

**Table 3**
Angles (°), screw translation and direction of rotation axis and point on rotation axis that define the change in quaternary structure between pairs of structures.

Values of $\theta_1$ and $\theta_2$ are highlighted in bold. The upper right part of the table contains the $\theta_1$ angles. The lower left part contains the $\theta_2$ angles and the screw translation (first row), the direction of the rotation axis (second row) and the point on the rotation axis (third row). Numbering is as in Table 2.

| | 1 | 2 | 3 | 4 | 5 | 6 | 7 | 8 |
|---|---|---|---|---|---|---|---|---|
| 1 | — | **0.7** | **0.4** | **2.5** | **3.0** | **2.4** | **5.8** | **6.8** |
| 2 | **1.5** (−0.1)<br>50.8, 89.9, 39.2<br>−19.2 −12.7 0.1 | — | **1.1** | **2.3** | **2.7** | **2.3** | **5.6** | **6.7** |
| 3 | **0.7** (0.2)<br>28.4, 89.9, 61.6<br>−12.0 9.9 −6.5 | **2.2** (0.1)<br>41.4, 90.0, 48.6<br>−9.7 8.5 −8.5 | — | **2.6** | **3.1** | **2.5** | **5.8** | **7.0** |
| 4 | **4.9** (0.2)<br>63.4, 90.0, 26.6<br>−1.4 −4.0 2.7 | **4.6** (−0.1)<br>46.9, 90.0, 43.1<br>−4.2 −4.6 4.5 | **5.2** (0.4)<br>70.8, 90.0, 19.2<br>−0.4 −4.9 1.3 | — | **0.5** | **0.0** | **3.3** | **8.9** |
| 5 | **5.9** (0.6)<br>64.4, 90.0, 25.6<br>−0.9 −4.9 2.1 | **5.9** (0.1)<br>53.1, 90.0, 36.9<br>−2.8 −6.7 3.7 | **6.3** (0.8)<br>72.6, 90.0, 17.4<br>−0.2 −5.2 0.6 | **1.1** (0.4)<br>83.1, 90.0, 6.9<br>0.2 −2.7 −1.4 | — | **0.6** | **2.8** | **9.4** |
| 6 | **4.9** (0.2)<br>64.9, 89.9, 25.1<br>−1.2 0.4 2.6 | **4.9** (0.0)<br>47.5, 90.0, 42.5<br>−4.0 −0.1 4.4 | **5.1** (0.4)<br>72.5, 90.0, 17.5<br>−0.3 −0.7 0.8 | **0.2** (0.3)<br>45.4, 90.0, 44.5<br>−19.3 −62.6 1.7 | **1.2** (−0.4)<br>73.7, 90.0, 16.3<br>−27.6 22.1 −7.4 | — | **3.2** | **9.1** |
| 7 | **11.7** (0.7)<br>67.9, 90.0, 22.1<br>−0.6 −4.7 1.5 | **11.6** (0.4)<br>62.2, 90.0, 27.8<br>−0.9 −5.4 1.8 | **11.7** (1.0)<br>70.8, 90.0, 19.2<br>−0.3 −5.0 0.8 | **6.7** (0.6)<br>71.7, 89.9, 18.3<br>−0.3 −4.5 0.8 | **5.6** (0.1)<br>70.0, 90.0, 20.0<br>−0.4 −4.1 1.1 | **6.4** (0.5)<br>62.2, 90.0, 27.8<br>−0.6 −7.9 1.6 | — | **12.1** |
| 8 | **13.6** (−2.2)<br>28.5, 90.0, 61.5<br>−17.9 11.9 −8.1 | **13.3** (−2.8)<br>35.2, 90.0, 54.8<br>−10.6 12.4 −10.0 | **14.1** (−2.0)<br>25.8, 90.0, 64.2<br>−17.6 10.7 −8.2 | **18.0** (−2.8)<br>38.1, 90.0, 51.9<br>−19.9 9.4 −8.8 | **18.7** (−3.1)<br>40.9, 90.0, 49.1<br>−20.6 9.8 −8.6 | **18.1** (−2.8)<br>38.8, 90.0, 51.3<br>−20.5 7.9 −9.3 | **24.2** (3.1)<br>43.5, 90.0, 46.5<br>−4.9 −8.7 4.7 | — |

r.h. 66% form are roughly midway between those in the R and the R2 states and are similar to that in low-salt horse methaemoglobin and in what is described as the RR2 state.

## 4. Discussion

The results presented here lend additional support to the conclusion that haemoglobin can access an ensemble of relaxed states. Most importantly, they show that a change in water content can cause a variation in the relaxed state. The R2 state was originally observed in liganded human haemoglobin at a comparatively low ionic strength and low pH. Thus, it appeared that these conditions would favour the R2 state (Silva *et al.*, 1992). Subsequently, three crystallographically independent molecules with quaternary structures intermediate between those of R and R2 were observed in human methaemoglobin crystals grown at low ionic strength but at the same pH used for crystallizing R-state human oxyhaemoglobin (Biswal & Vijayan, 2001). Simultaneously, other liganded haemoglobin structures with quaternary associations between those corresponding to R and R2 were reported (Mueser *et al.*, 2000). Recently, in a set of very interesting results, crystals containing human carbonmonoxyhaemoglobin molecules in a state intermediate between R and R2 (designated RR2) and those with molecules in a new liganded state (R3) have been grown under the conditions in which crystals of R-state haemoglobin were grown (Safo & Abraham, 2005). Thus, the ionic strength and the pH of the medium cannot be directly correlated with the nature of the liganded states. However, it is clear that variation in them cause shifts in the quaternary structure among the various possibilities. The work reported here suggests that changes in water content also cause variations in the quaternary structure of liganded haemoglobin.

Attempts have been made previously to explore the variation in quaternary structure as a function of water content in crystals of human oxyhaemoglobin and horse methaemoglobin. However, in these investigations the crystals only remained stable within a range of 2–3 percentage points of solvent content. In the present study, however, crystal structures with fairly large variations in solvent content could be examined. The results indicate that for a given crystal packing, removal of water leads to a movement from R towards R2. The native R and the r.h. 79% forms have the same crystal packing, but the water content of the r.h. 79% form is substantially lower. Presumably, as a result of the loss of water, the quaternary association of the molecules in the r.h. 79% form moves slightly towards that in the R2 state, at least as far as the mutual disposition of the two $\alpha\beta$ dimers is concerned. The crystal packing changes somewhat during the water-mediated transformation between r.h. 79% and r.h. 75%. Although the transformation is caused by a reduction in the environmental humidity, it is accompanied by the uptake of water. The water content of the native R and r.h. 75% forms is now comparable and so are their quaternary structures. Crystal packing in the r.h. 75% and r.h. 66% forms is similar but not identical. However, the water content in the latter is substantially lower and indeed the quaternary structure of the molecules in the r.h. 66% form is intermediate between those in the R and the R2 states. The movement towards R2 is not linearly related to the degree of dehydration. The r.h. 79% and r.h. 66% forms have nearly the same water content, but the quaternary structure in the latter is closer to R2 than that in the former. Thus, the effect of the change in water content is modulated by other factors such as differences in crystal packing.

As mentioned previously, we have demonstrated through detailed investigations that in simpler systems such as lysozyme and ribonuclease A, the changes in the molecular geometry resulting from

partial dehydration are similar to those that occur during substrate binding. Very recently, we have also demonstrated that the removal of water from crystals of $\beta$-lactoglobulin results in the closure of a hydrophobic pocket through the movement of a loop, as happens when the protein binds an appropriate ligand. Thus, movements resulting from a change in water content appear to mimic those involved in protein action. In this context, the changes in quaternary structure observed in the present study are interesting. It is believed that R2 is an end state of liganded haemoglobin and that the path to it from the T state is through the R state. Partial dehydration appears to help the molecule along this path.

Data were collected at the X-ray Facility for Structural Biology at the Molecular Biophysics Unit supported by the Department of Science and Technology, Government of India. Computations were performed at the Supercomputer Education and Research Centre and the Bioinformatics Centre and the Graphics Facility, both supported by the Department of Biotechnology (DBT). This work was supported by the Council of Scientific and Industrial Research (CSIR). PSK is a CSIR research fellow. MV is supported by a Distinguished Biotechnologist Award from the DBT.

## References

Baldwin, J. M. (1980). *J. Mol. Biol.* **136**, 103–128.
Baldwin, J. M. & Chothia, C. (1979). *J. Mol. Biol.* **129**, 175–220.
Biswal, B. K., Sukumar, N. & Vijayan, M. (2000). *Acta Cryst.* D**56**, 1110–1119.
Biswal, B. K. & Vijayan, M. (2001). *Curr. Sci. (India)*, **81**, 1100–1105.
Biswal, B. K. & Vijayan, M. (2002). *Acta Cryst.* D**58**, 1155–1161.
Brünger, A. T., Adams, P. D., Clore, G. M., DeLano, W. L., Gros, P., Grosse-Kunstleve, R. W., Jiang, J.-S., Kuszewski, J., Nilges, M., Pannu, N. S., Read, R. J., Rice, L. M., Simonson, T. & Warren, G. L. (1998). *Acta Cryst.* D**54**, 905–921.
Brzozowski, A., Derewenda, Z., Dodson, E. & Dodson, G. (1984). *Nature (London)*, **307**, 74–76.
Cohen, G. E. (1997). *J. Appl. Cryst.* **30**, 1160–1161.
Collaborative Computational Project, Number 4 (1994). *Acta Cryst.* D**50**, 760–763.
DeLano, W. L. (2002). *The PyMOL Molecular Graphics System.* http://www.pymol.org.
Fermi, G., Perutz, M. F., Shaanan, B. & Fourme, R. (1984). *J. Mol. Biol.* **175**, 159–174.
Jones, T. A., Zou, J.-Y., Cowan, S. W. & Kjeldgaard, M. (1991). *Acta Cryst.* A**47**, 110–119.
Huxley, H. E. & Kendrew, J. C. (1953). *Acta Cryst.* **6**, 76–80.
Kodandapani, R., Suresh, C. G. & Vijayan, M. (1990). *J. Biol. Chem.* **265**, 16126–16131.
Kraulis, P. J. (1991). *J. Appl. Cryst.* **24**, 946–950.
Kuriyan, J., Wilz, S., Karplus, M. & Petsko, G. A. (1986). *J. Mol. Biol.* **192**, 133–154.
Laskowski, R. A., Moss, D. S. & Thornton, J. M. (1993). *J. Mol. Biol.* **23**, 1049–1067.
Liddington, R., Derewenda, Z., Dodson, E., Hubbard, R. & Dodson, G. (1992). *J. Mol. Biol.* **228,** 551–579.
Madhusudan, Kodandapani, R. & Vijayan, M. (1993). *Acta Cryst.* D**49**, 234–245.
Madhusudan & Vijayan, M. (1991). *Curr. Sci. (India)*, **60**, 165–170.
Matthews, B. W. (1968). *J. Mol. Biol.* **33**, 491–497.
Merritt, E. A. & Bacon, D. J. (1997). *Methods Enzymol.* **277**, 505–524.
Monod, J., Wyman, J. & Changeux, J. P. (1965). *J. Mol. Biol.* **12**, 88–118.
Mueser, T. C., Rogers, P. H. & Arnone, A. (2000). *Biochemistry*, **39**, 15353–15364.
Murshudov, G. N., Vagin, A. A. & Dodson, E. J. (1997). *Acta Cryst.* D**53**, 240–255.
Nagendra, H. G., Sudarsanakumar, C. & Vijayan, M. (1996). *Acta Cryst.* D**52**, 1067–1074.
Nagendra, H. G., Sukumar, N. & Vijayan, M. (1998). *Proteins*, **32**, 229–240.
Navaza, J. (1994). *Acta Cryst.* A**50**, 157–163.
Otwinowski, Z. & Minor, W. (1997). *Methods Enzymol.* **276**, 307–326.
Park, S. Y., Yokoyama, T., Shibayama, N., Shiro, Y. & Tame, J. R. (2006). *J. Mol. Biol.* **360**, 690–701.
Perutz, M. F. (1954). *Proc. R. Soc. London Ser. A*, **225**, 264–286.
Perutz, M. F. (1968). *J. Cryst. Growth*, **2**, 54–56.
Perutz, M. F. (1970). *Nature (London)*, **228**, 726–739.
Perutz, M. F., Wilkinson, A. J., Paoli, M. & Dodson, G. G. (1998). *Annu. Rev. Biophys. Biomol. Struct.* **27**, 1–34.
Radha Kishan, K. V., Chandra, N. R., Sudarsanakumar, C., Suguna, K. & Vijayan, M. (1995). *Acta Cryst.* D**51**, 703–710.
Sadasivan, C., Nagendra, H. G. & Vijayan, M. (1998). *Acta Cryst.* D**54**, 1343–1352.
Safo, M. K. & Abraham, D. J. (2005). *Biochemistry*, **44**, 8347–8359.
Salunke, D. M., Veerapandian, B., Kodandapani, R. & Vijayan, M. (1985). *Acta Cryst.* B**41**, 431–436.
Sankaranarayanan, R., Biswal, B. K. & Vijayan, M. (2005). *Proteins*, **60**, 547–551.
Schumacher, M. A., Zheleznova, E. E., Poundstone, K. S., Kluger, R., Jones, R. T. & Brennan, R. G. (1997). *Proc. Natl Acad. Sci. USA*, **94**, 7841–7844.
Shaanan, B. (1983). *J. Mol. Biol.* **171**, 31–59.
Silva, M. M., Rogers, P. H. & Arnone, A. A. (1992). *J. Biol. Chem.* **267**, 17248–17256.
Srinivasan, R. & Rose, G. D. (1994). *Proc. Natl Acad. Sci. USA*, **91**, 11113–11117.
Sukumar, N., Biswal, B. K. & Vijayan, M. (1999). *Acta Cryst.* D**55**, 934–937.
Vásquez, G. B., Ji, X., Fronticelli, C. & Gilliland, G. L. (1998). *Acta Cryst.* D**54**, 355–366.
Vijayalakshmi, L., Krishna, R., Sankaranarayanan, R. & Vijayan, M. (2008). *Proteins*, **71**, 241–249.
West, R. C. & Astle, M. J. (1980). *CRC Handbook of Chemistry and Physics*, 61st ed., p. E-46. Boca Raton: CRC Press.